# Model Estimates of the Mass Balance of the Greenland and Antarctic Ice Sheets

Véronique Bugnion

**Abstract**

The six possible combinations of two climate models and three methods for calculating the melting of snow and ice are used to estimate current values of accumulation and ablation on the Greenland and Antarctic ice sheets. This allows the contrasting of high vs. low resolution climate input and to assess the reliability of simple temperature based parameterizations of melting when compared to a physical model of the seasonal evolution of the snow cover. In contrast to past efforts at modelling the mass balance of Greenland and Antarctica, the latter model allows an explicit calculation of the formation of meltwater, of the fraction of meltwater which refreezes and of runoff in the ablation region, this is not the case for the other two melt models. While the higher resolution GCM (ECHAM 4) does bring the estimation of accumulation closer to observations, it fails to give accurate results in its predictions of runoff. The simpler climate model (MIT 2D LO) overestimates accumulation in Antarctica but produces satisfactory estimates of runoff from the Greenland ice sheet. Both models reproduce some of the characteristics of the extent of the wet snow zone observed with satellite remote sensing, but the MIT model is closer to observations in terms of areal extent and intensity of the melting. The temperature dependent melting parameterizations generally require an accuracy in the climatic input beyond what is currently achieved to produce reliable. Because it is based on physical principles and relies on the surface energy balance as input, the snow cover model is believed to have the capability to respond adequately to the current climatic forcing as well as to future changes in climate.

# 1 Introduction

Greenland and Antarctica contain together over 99% of the volume of glacier ice on Earth or about 75 meters of sea-level equivalent, yet the current state of the mass balance of these ice sheets, let alone how it may evolve in the future, is poorly known. The estimated contribution of those two ice sheets to the sea level rise of the past century reflects these uncertainties: The Houghton et al. (1996) report gives a central value of $0\,cm$, with the uncertainty range estimated at $\pm 4\ cm$ for Greenland and $\pm 14\ cm$ for Antarctica.

The two most important processes determining the mass balance at the surface of an ice sheet are snow accumulation and the runoff of meltwater. The accumulation in Antarctica is balanced almost entirely by the calving of icebergs, Greenland however balances accumulation by approximately equal amounts of iceberg calving and runoff.

Because of the volumes of ice involved, even small modifications in the mass balance of these ice sheets will be of crucial importance to future changes in the level of the oceans. Obtaining reliable estimates of short-term changes in mass balance does however require climate models which capture adequately the essential features of the current Arctic and Antarctic climate, and snow and ice melt models which can be trusted to estimate melting and runoff accurately. This paper addresses both issues by combining climate and melt models of varying complexity and assessing the reliability of the results. The three melt models which will be used to estimate the runoff from Greenland and the extent of the melt zone in Antarctica are described in section 2, with particular focus on a new approach to capturing changes in the snow cover. The climatic forcing is derived from the output of current climate simulations performed with two climate models of substantially different complexity, the MIT 2D-LO and ECHAM 4 models. Section 3 focuses on the climatology of key variables such as accumulation, temperature and albedo produced by these two models. Section 4 assesses the performance of the combined climate – melt models by comparing the results obtained at individual sites with measured meteorological and ablation data, and by comparing the extent of the "wet snow" zone with a similar quantity derived from satellite remote sensing measurements. The estimates of runoff integrated over the entire ice sheets are compared to the best guess derived from field data and discussed in section 5. An

outlook on the perspective for modeling future changes in the mass balance of Greenland and Antarctica is found in the conclusion.

# 2 Melt Models

Two temperature-based parameterizations which have been used in the past to estimate the runoff from snow and ice covered surfaces are briefly presented. The results obtained with these simple models will be contrasted with those derived with a more complicated, physically based, approach.

The three models are solved on both 40 $km$ and 20 $km$ grids over the Greenland ice sheet and a 40 $km$ grid over Antarctica. This high resolution is required in order to obtain realistic estimates of ablation, Glover (1999) argues that this is due to a more accurate representation of the topography of the ice sheets and in particular of the steeply sloping coastal regions.

## 2.1 Runoff Parameterizations

The simplest parameterization, called here the linear model, relies on the observed correlation between the summer ablation, in meters, and the average summer temperature, $T_{avg}$, for $T_{avg} > -2°C$ (Wild and Ohmura, 1999):

$$\text{Runoff} = 0.514 \cdot \text{T}_{\text{avg}} + 0.93 \tag{1}$$

The coefficients were obtained by performing a linear regression between the ablation and the summer temperature. This model has the advantage of simplicity, yet the drawback of neglecting the influence of a number of factors on melting. The non-linear evolution of the surface albedo for air temperatures near and above the melting point and the differences in albedo between snow and ice (Kang, 1994) can for example be expected to undermine the assumption of a linear behavior underlying this model.

A slightly more sophisticated temperature based parameterization is commonly referred to as a degree-day model (Braithwaite and Olesen, 1989; Huybrechts et al., 1989). It relies on the integral of the positive air temperatures over the summer, positive degree-days or PDD, as melting potential and introduces two different melting factors for snow and ice

in an attempt to represent the differences in the albedos of these two surfaces. The snow accumulated during the winter is melted first at the rate $m_{snow} = 0.03$ m/PDD. A prescribed fraction of that meltwater, $P_{max} = 0.6$, refreezes to form superimposed ice layers. The remainder of the positive degree-days are used to melt ice at the rate $m_{ice} = 0.08$ m/PDD, this meltwater contributes to the runoff from the ice sheet. The melt rates, $m_{snow}$ and $m_{ice}$, have been shown to vary with location on the ice sheet (Braithwaite, 1995), they will be kept constant in this study to test the universality of the parameterization and allow a comparison with previous model studies.

## 2.2 Snowpack model

A complete approach to modeling the temperature and density distribution of a snow, firn and ice mixture would require a three phase, four-component system: Liquid water, water vapor, ice and air (Morland et al., 1990). Simplified models with two or three components have been developed for avalanche forecasting purposes in the Alps (Brun et al., 1989; Bader and Weilenmann, 1992) or to describe the evolution of the seasonal snowcover (Anderson, 1976; Loth and Graf, 1993). A similar modeling approach is used here to estimate the mass balance of the Greenland and Antarctic ice sheets. Because snowpack models are based on physical principles, it is believed that their response to changes in the climatic forcing is appropriate. This is not the case for parameterizations which are calibrated to a certain range of climatic conditions.

The model described in the following paragraphs is one-dimensional in the vertical direction, it treats the uppermost 15 meters of the snow/firn/ice as a two component system: Liquid water and snow. Ice and air are treated jointly as snow of variable density. Although the firn air is saturated with water vapor, the contribution of sublimation/fusion to the energy and mass balances can be shown to be negligible (Bader and Weilenmann, 1992). Liquid water can only be present if the snow is at the melting point and is absent at lower temperatures. This common temperature of the water/snow mixture presents the advantage of reducing the problem to a single thermodynamic equation for both components.

The momentum balance for snow can be reduced to a hydrostatic balance with the

atmospheric pressure serving as surface boundary condition. The constitutive relation for snow – relation between the deformation or strain rate and the imposed stress – is derived from observations of the rate at which snow settles under the pressure of the overlying layers. Snow is best described as a compressible viscoelastic material in which the viscosity is both density and temperature dependent (Male, 1980). This yields the following rate of change in the thickness, $h$, of a layer of snow:

$$\frac{d}{d\,z}\left(\frac{d\,h}{d\,t}\right) = \frac{\sigma_s}{\eta} \tag{2}$$

$$\eta(T, \rho_s) = 5.38 \cdot 10^{-3} e^{0.024\rho_s + \frac{6042}{T}} \tag{3}$$

where the temperature $T$ is in Kelvin and $\sigma_s$ is the snow load. The compaction viscosity, $\eta$, which is used in this model was derived empirically from measurements in Greenland and Antarctica (Male, 1980; Morris et al., 1997). Although small, the vertical velocity due to snow settling, $w_s$, can easily be retrieved from the change in layer depth.

Two mass conservation equations for the density of snow, $\rho_s$, and its water content, $\theta$, are required to translate the phase changes between the components into density changes.

$$\frac{d\rho_s}{d\,t} = \frac{\partial \rho_s}{\partial t} + w_s \frac{\partial \rho_s}{\partial z} = -m_{s-w} \tag{4}$$

$$\frac{d\theta}{d\,t} = m_{s-w} \tag{5}$$

$m_{s-w}$ is the melting rate per unit volume.

The mass balance for liquid water must take into account the percolation of water between the layers. Drainage is modeled by a simple maximum retention capacity model: The water in excess of a prescribed volume fraction percolates to the lower layer. The reference value chosen for this so-called "irreducible water saturation" is 3% per unit volume (Male, 1980). A more complicated Darcy type flow law as the one proposed by Colbeck (1972) would be more accurate but its implementation requires a timestep too short for our modeling objectives. Horizontal movement of the meltwater is neglected on the grounds that any liquid water flowing down the slope of the ice sheet will generally encounter areas in which the firn is already saturated with water and will not refreeze. Once formed, the runoff is therefore assumed to reach the ocean.

The snowpack model is initialized by prescribing a uniform temperature distribution and a density profile increasing linearly from the surface to $15m$ depth. The time taken for the snow cover to equilibrate with the current climate and develop realistic density and temperature profiles varies with the location on the ice sheet and can take up to a century.

Fig.1 represents the seasonal evolution of two density profiles, one at the Carrefour site in the accumulation zone (left-hand figure), the other at Nordbogletscher in the ablation area of the Greenland ice sheet. These profiles were obtained by using the surface forcing of the MIT climate model's representation of the current climate (see Section 3 for a description of the climate models). The density increase in the accumulation zone is gradual and the transition to ice occurs below $15\,m.$, at depths between 40 and 115 $m$ depending on the accumulation rate and the surface temperature (Paterson, 1994). Fresh snow is added at a density of $320\,kg\,m^{-3}$, a value which is usually reached in polar snow after less than a day of settling (Morris et al., 1997). In the ablation region (right-hand figure), the ice is covered with a thin cover of snow which gradually thickens during the fall, winter and spring seasons. As shown by the July curve (dash-dotted line), bare ice is exposed at the surface during the summer.

The temperature, $T$, within the snow pack is determined by heat diffusion and by the changes of phase of water.

$$Cp_{\mathit{eff}}\frac{\partial T}{\partial t} = \frac{\partial}{\partial z}\lambda_{\mathit{eff}}\frac{\partial\, T}{\partial z} + L_{s-w}\cdot m_{s-w} \tag{6}$$

The effective heat capacity, $Cp_{\mathit{eff}}$, and thermal conductivity, $\lambda_{\mathit{eff}}$, take into account the mass fraction of snow and water in the mixture. $L_{s-w}$ is the latent heat of fusion and $m_{s-w}$ represents the mass of water per unit volume which changes phase at a given timestep. A scale analysis of the generalized thermodynamic equation shows that the advection of heat by snow settling or water percolation is smaller than the other terms. The penetration of shortwave radiation in the snowpack is attenuated completely within the uppermost centimeters of the snow, and has therefore been neglected, as has the effect of wind pumping on the sensible heat loss within the snowpack.

This diffusion equation being of second order in space, two boundary conditions are required to obtain a solution. Since the annual temperature cycle is damped within the

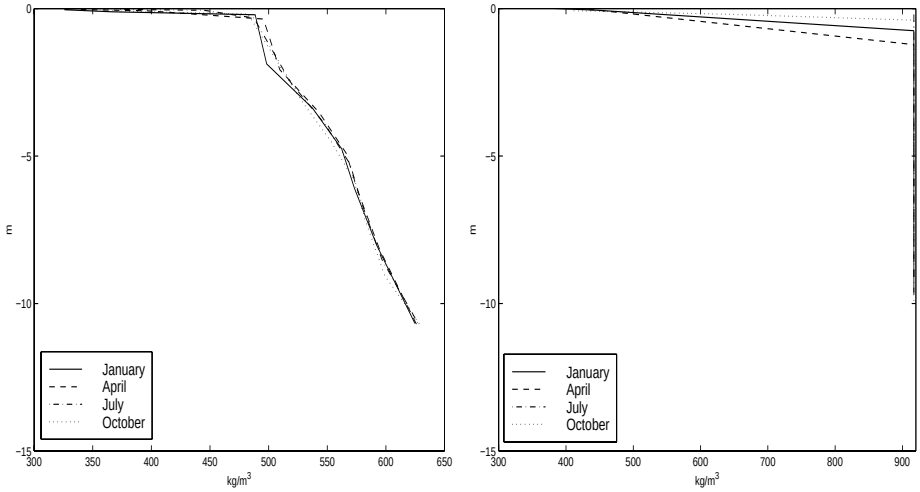


Figure 1: Model depth Profiles (in $m$) of the snow/ice density (in $kg\,m^{-3}$) for January, April, July and October. Left: Carrefour ($69°50'N; 45°25'W; 1850\ m$, Greenland). Right: Nordbogletscher ($61°28'N; 45°20'W; 880\ m$, Greenland). The figures are plotted on different scales for clarity. The climate forcing is derived from the MIT model simulation of the 1990 climate.

uppermost meters of the snowpack, a vanishing heat flux at $15\,m$ depth provides an excellent lower boundary condition, even when integrating the model forward over a century. The surface energy balance – sum of the net shortwave $Q_{SW}$ and longwave $Q_{LW}$ radiative fluxes and of the turbulent latent $Q_{LAT}$ and sensible $Q_{SENS}$ heat fluxes – can be used to calculate the heat flux through the surface of the ice sheet:

$$\lambda_{eff} \left.\frac{\partial T}{\partial z}\right|_{z=0} = Q_{SW} + Q_{LW} + Q_{LAT} + Q_{SENS} \tag{7}$$

The downwelling shortwave radiation must be available from measurements or from an atmospheric model output. The net absorbed shortwave radiation can be determined if the surface albedo, $\alpha$, is known or prescribed. The albedo parameterization used in this model includes a dependence on the time elapsed, $t$ here in days, since the previous snowfall (Loth and Graf, 1993),

$$\begin{aligned} \alpha(t) &= \alpha_0 - 0.0061 \cdot t \qquad \text{no melting} \\ \alpha(t) &= \alpha_0 - 0.015 \cdot t \quad \text{melting period} \end{aligned} \tag{8}$$

and takes advantage of the strong correlation between the albedo of snow and ice and the air

temperature (Kang, 1994). Ice is assumed to have a constant albedo (Knap and Oerlemans, 1996):

$$\begin{aligned} \alpha_0 &= 0.88 - 6 \cdot 10^{-3} \cdot T_{air} && -10 < T_{air} < 0°C && \text{cold snow} \\ \alpha_0 &= 0.82 - 0.03 \cdot T_{air} - 1.74 \cdot 10^{-3} \cdot T_{air}^2 - 1.14 \cdot 10^{-4} \cdot T_{air}^3 && 0 < T_{air} < 8°C && \text{temperate snow} \\ \alpha_0 &= 0.44 && && \text{ice} \end{aligned} \tag{9}$$

The upwelling longwave radiation can be calculated by assuming that the snow cover emits as a blackbody, the downwelling component must be provided as input.

The latent and sensible heat fluxes are parameterized with the bulk transfer formulae described in Hansen et al. (1983) and Sokolov and Stone (1995). Different roughness lengths for cold, temperate snow and ice, $z_{cold\ snow} = 0.12 \cdot 10^{-3}\ m$, $z_{temperate\ snow} = 1.3 \cdot 10^{-3}\ m$ and $z_{ice} = 3.2 \cdot 10^{-3}\ m$ are used in the calculation of the bulk transfer coefficients (Greuell, 1992). The assumption of a constant 70% relative humidity is used to derive the air specific humidity required for the calculation of the latent heat flux. Although this value is lower than most reports by stations located near the coast, it is not inconsistent with values measured inland (Schwerdtfeger, 1970). It furthermore gives latent heat fluxes which are in agreement with observations.

The seasonal variation of two temperature profiles on the Greenland ice sheet, as predicted by the snowpack model for the current climate, are shown in Fig.2. There is a strong coupling between the surface snow temperature and the air temperature at the Carrefour site in the accumulation zone (left-hand figure), and the annual temperature cycle is rapidly damped with depth. The convergence of the seasonal temperature profiles by a depth of $10\,m$ validates the use of a vanishing heat flux at $15\,m$ as lower boundary condition. The profiles on the right-hand side of Fig.2 are representative of the ablation zone (Norbodgletscher). The uppermost centimeters of the snow/water mixture in the July profile (dash-dotted line) are temperate while the lower part remains below the freezing point. The temperature inversion which develops in October is a common characteristic of both temperature profiles.

The numerical procedure used to calculate the temperature distribution is the Crank-Nicholson scheme which is unconditionally stable for a dry snowpack, yet requires the convergence procedure described by Bader and Weilenmann (1992) to ensure an accurate cal-

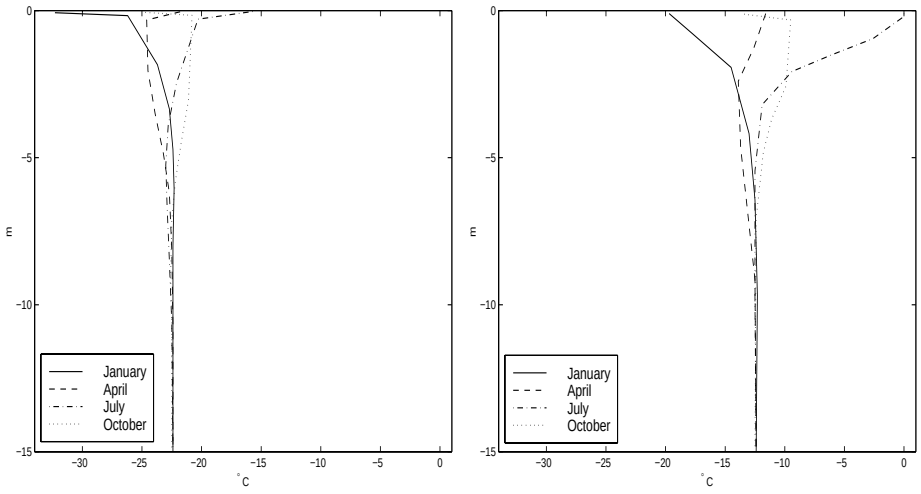


Figure 2: Model depth Profiles (in $m$) of the snow/ice temperature (in $^{\circ}C$) for January, April, July and October. Left: Carrefour ($69^{\circ}50'N; 45^{\circ}25'W; 1850\ m$, Greenland). Right: Nordbogletscher ($61^{\circ}28'N; 45^{\circ}20'W; 880\ m$, Greenland). The climate forcing is derived from the MIT model simulation of the 1990 climate.

culation of the mass of water which is melted or frozen at each timestep. The timestep is determined individually at each grid point by the total amount of melting experienced during the previous year. This guarantees an optimal accuracy for the points in the ablation zone which require a shorter timestep because of melting and percolation and an efficient scheme in the accumulation zone. The timestep therefore varies between 1 hour and 1 day depending on the location on the ice sheet.

Snow or ice of a density and temperature equivalent to that of the lowest model layer is added or subtracted to the column at each timestep in order to maintain a constant total thickness of $15\,m$. Because of the snow settling process, the layers do not maintain a constant thickness and are combined or divided at every timestep to ensure smooth density and temperature profiles.

# 3 Performance of the climate models in capturing the climate of the ice sheets

Snow melt models are ideally tested by providing as input observed meteorological data and comparing the predicted and observed ablation. There are however no stations in the ablation region of the Greenland ice sheet which provide year-round measurements of all the meteorological parameters required for the snowpack model. The two climate model simulations which were therefore used as input to the melt models are the current climate representations obtained with the ECHAM 4 GCM (Wild and Ohmura, 1999) and the MIT 2D-LO model (Sokolov and Stone, 1995, 1998). The ECHAM model is a three-dimensional climate GCM which was run at very high resolution (T106 or $1.1^\circ \times 1.1^\circ$) in order to adequately resolve the topographic features of the Greenland and Antarctic ice sheets. The simulation was performed by using the sea surface temperature and sea-ice distribution predicted by a coarser resolution simulation with the same model (Roeckner et al., 1999) as lower boundary conditions for a 10 year integration of the high resolution version. The MIT 2D-LO model is a zonally averaged, height vs. latitude, version of the GISS GCM (Hansen et al., 1983). The model does however distinguish between land, ocean land-ice and sea-ice in each latitude band and has a resolution of $7.8^\circ$ in latitude. Because it has no topography, certain climatic input fields had to be adjusted, as described later, in order to obtain realistic distributions over the ice sheets. The advantage of the ECHAM model is its high resolution and physics, yet the simplicity of the MIT model allows the simulation of a range of transient climate change experiments which are described in a companion paper (Bugnion, 1999). The input variables from the climate models are: The downwelling shortwave and longwave radiation, wind speed, surface air temperature and the precipitation. They are interpolated onto the $20/40\,km$ grid of the snow melt models.

Because the input data from the climate models was available as monthly means and the snowpack model's timestep is much shorter, random gaussian variability was added to the temperature ($\sigma_T = 2^\circ C$) and wind records ($\sigma_{\vec{v}} = 4\,m/s$) to ensure an adequate climate variability. The precipitation was disaggregated into individual events with a simple

stochastic rainfall model in order to allow the albedo to depend upon the time elapsed since the previous snowfall event. This model performs a random selection between a set of precipitation events of predertermined duration and intensity.

The reliability of the representation by those two climate models of the climate of the ice sheets is assessed in the following paragraphs by comparing the predicted mass and energy balance components to observations.

## 3.1 Accumulation

The ECHAM model generally reproduces well the local features of the accumulation pattern over Greenland and Antarctica (Wild and Ohmura, 1999). The precipitation field derived from the MIT model is obtained by multiplying the zonal average precipitation amount with an array consisting of the observed snow accumulation over the ice sheet, normalized over each latitude band in order to conserve the amount of precipitation predicted by the climate model. The total snow accumulation integrated over the ice sheets predicted by the two climate models and the measured estimates are summarized in Table 1. Because the observed accumulation is for the most part derived from snow pit measurements and not from rain or snow gauge data, the evaporation estimated by the snowpack model is subtracted from the model's total snowfall before comparing it to the observed accumulation. The snow accumulation predicted for the Greenland ice sheet is within the range of uncertainty of observations for both climate models. The high resolution of the ECHAM model does however allow some improvement over the value predicted by the MIT model in Antarctica but both are significantly higher than the most recent observations (Vaughan et al., 1999). Note that the accumulation calculated on the original ECHAM 4 T106 grid by using that model's snowfall and evaporation is 20% smaller than the number obtained on the 40 km grid (Wild and Ohmura, 1999). The difference stems from the larger evaporation calculated by the ECHAM model when compared to the snowpack model and from differences in snowfall in the coastal areas of the continent which are due to the interpolation procedure and the resolution. As noted by Genthon (1994), the overestimate of precipitation in high latitudes is a problem encountered by many GCM's. In the case of the MIT model, the excess precipitation in

Antarctica is to some degree due to the absence of topography. This allows the surface temperatures and specific humidities to be higher than they should, thereby leading to excessive precipitation. Adding the zonally averaged topography of Antarctica at the model's lower boundary does in fact reduce the total accumulation by 15%. The second source of error is associated with the presence of a vertical wall at the southernmost grid point. This wall induces excessive upward motion and precipitation. This is a problem specific to two-dimensional models which is not encountered by their three-dimensional counterparts.

| | Greenland | | | Antarctica | | |
|---|---|---|---|---|---|---|
| | Snowfall | Evaporation | Accumulation | Snowfall | Evaporation | Accumulation |
| MIT | 649 | 95 | 554 | 3121 | 246 | 2875 |
| ECHAM 4 | 585 | 46 | 540 | 2732 | 241 | 2491 |
| Observations | Ohmura & Reeh, 91 | | 535 | Budd & Smith, 85 | | 1800 |
| | Reeh, 94 | | 553 | Bentley & Giovinetto, 91 | | 1660 |
| | | | | Jacobs & al., 92 | | 1528 |
| | | | | Vaughan & al., 99 | | 1810 |

Table 1: Model predicted total snowfall, evaporation and accumulation. Source for the observations are Houghton et al. (1996) and Vaughan et al. (1999). Units are $10^{12} kg\, a^{-1}$

The estimates of snowfall and evaporation and thus accumulation are virtually unaffected by the choice of the grid resolution, 40 or 20 $km$, on the Greenland ice sheet.

## 3.2 Temperature

The air temperature is extrapolated from the climate model's topography to the true elevation by using a seasonally varying lapse rate (Ohmura, 1987; Schwerdtfeger, 1970). This is particularly important for the MIT model which resolves land and ocean but has no topography; the correction applied to the ECHAM data is small and does not significantly affect the results. This simple adjustment allows an excellent reconstruction of the annually averaged temperature distribution over the ice sheet. Figure 3 compares the temperature

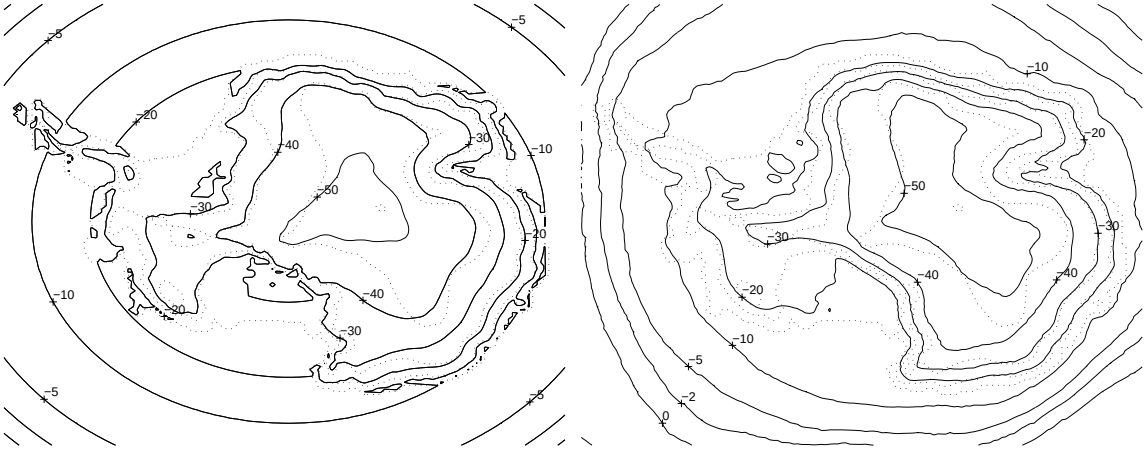

Figure 3: Model predicted (MIT - left, ECHAM 4 - right) annual mean temperature for Antarctica. Source for the ECHAM data Wild and Ohmura (1999). Units are $^{\circ}C$. The $1000\,m$. contours are plotted as dotted lines.

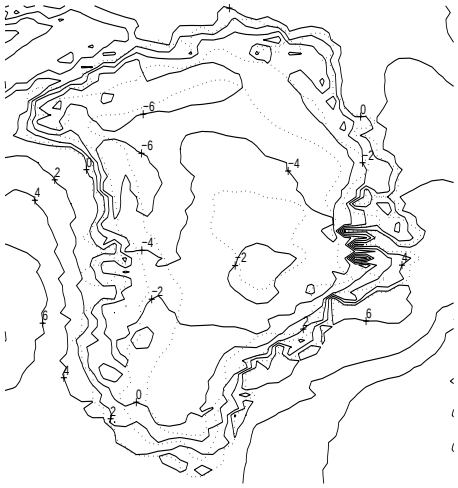

Figure 4: Difference (MIT - ECHAM) beteen the average summer temperature (June, July, August) predicted by the MIT and ECHAM models for Greenland. Source for the ECHAM data is Wild and Ohmura (1999) Units are $^{\circ}C$. The $1000\,m$. contours are plotted as dotted lines.

predicted by the MIT model with that of the ECHAM model, the latter has been shown by Wild and Ohmura (1999) to be close to observations.

Because summer temperatures determine directly the ablation and runoff predicted by the positive degree-day and linear models and indirectly the melting calculated by the snowpack model through their control of the snow albedo, they play a much more important role than the annual average temperature on the Greenland ice sheet. Fig.4 shows the difference between the average summer temperature (June, July, August) predicted by the MIT and ECHAM. The ECHAM model is 4–6 $^{\circ}C$ warmer than the MIT model in the Northern half of the ice sheet, and a few degrees colder in the Southern coastal regions. The comparison to the monthly mean temperature maps derived from observations (Ohmura, 1987) show the $5^{\circ}C$ isotherm at sea-level at about $74^{\circ}N$ and the $0^{\circ}C$ isotherm remaining fairly close to the coast along the northern shore, a situation in between what the two climate models are predicting.

## 3.3 Albedo

The albedo calculated by the snowpack model plays a crucial role in determining the amount of meltwater formed on the ice sheet. The value of 0.88 used for fresh snow and the prescribed dependence on the time elapsed since the previous precipitation event are adequate. This is confirmed by the comparison between model predicted and observed albedo shown in Fig.5 for two sites in the accumulation region of the ice sheets, Carrefour ($1850\,m.$) in Greenland and South Pole ($2835\,m.$) in Antarctica. The natural variability seems to be underestimated, perhaps because factors such as the diurnal variations of the solar zenith angle are neglected in the parameterization or because the stochastic rainfall model underestimates the natural variability.

The albedo parameterization near and above the melting point depends entirely on the surface air temperature. The good agreement between the predicted and observed temperatures and albedo shown in Fig.6 for the ETH station allows us to conclude that the albedo parameterization in the -8–4 $^{\circ}C$ range is adequate.

The absence of such high quality data for stations situated in the zone of extensive sum-

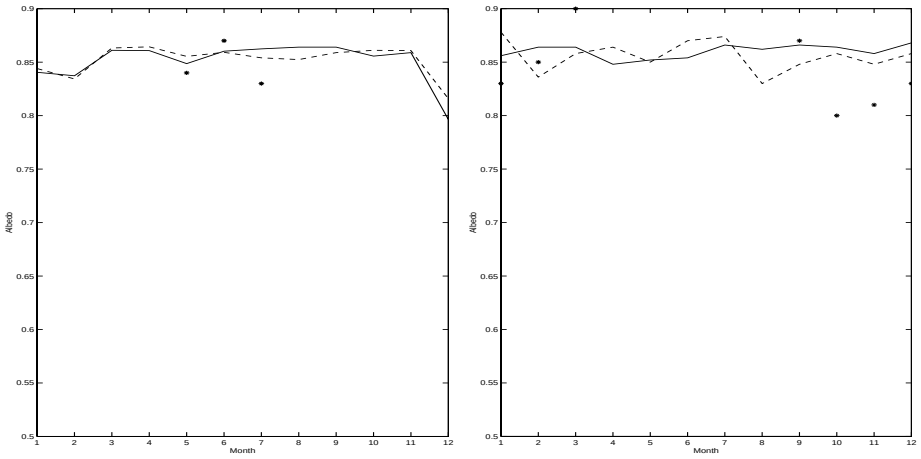


Figure 5: Seasonal variation of the snow albedo. Left: Carrefour site ($69°50'N; 45°25'W; 1850\ m$, Greenland). Right: South Pole station ($1850\,m.$, Antarctica). Full line: MIT model, Dashed line: ECHAM model, $*$: observations. Source for the observed is Gilgen and Ohmura (1999)

| | $\overline{T}_{obs}$ | $\overline{SW}_{obs}$ | $\overline{T}_{MIT}$ | $\overline{\alpha}_{MIT}$ | $\overline{SW}_{MIT}$ | $\overline{T}_{ECHAM}$ | $\overline{\alpha}_{ECHAM}$ | $\overline{SW}_{ECHAM}$ |
|---|---|---|---|---|---|---|---|---|
| Nordbogletscher | $\sim$4 | 111 | 5.4 | 0.56 | 106 | -0.6 | 0.85 | 27 |
| Qamanârssûp Sermia | $\sim$5 | 131 | 5.4 | 0.56 | 102 | 2.3 | 0.73 | 44 |

Table 2: Comparison between observed and model simulated mean summer temperature (June, July, August), in $°C$, albedo and net shortwave radiation, in $W\,m^{-2}$ at Nordbogletscher ($61°28'N; 45°20'W; 880\ m$, Greenland) and Qamanârssûp Sermia ($64°28'N; 49°50'W; 790\ m$, Greenland).

mer melting complicates the verification process in the 4–8 $°C$ temperature range. Table 2 compares the mean summer temperature and albedo at two sites which experience significantly more melting than the ETH station. The temperatures simulated by the MIT model are slightly too high at Nordbogletscher which will lead to an overestimation of the ablation, they are however generally close to observations. The good agreement between the observed net shortwave radiation, a quantity which is to a large extent determined by the surface albedo, and the values predicted by the MIT model confirm that the albedo parameterization is adequate (the underestimation of the net shortwave radiation at Qamanârssûp

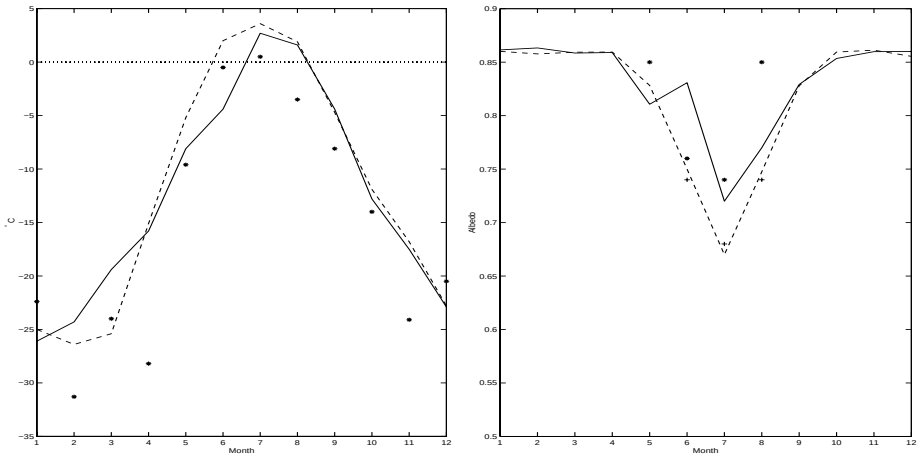


Figure 6: Seasonal variation of the air temperature (left) and snow albedo (right) at the ETH station ($69°34'N; 49°17'W; 1155\ m$, Greenland). Full line: MIT model, Dashed line: ECHAM model, $*(1990), +(1991)$: observations. Source for the observed is Gilgen and Ohmura (1999) and Ohmura et al. (1992).

Sermia is more likely to be due to an underestimation of the downwelling solar radiation at the surface by the MIT model at that site than to an overestimation of the albedo). The ECHAM model simulates temperatures which are too cold by several degrees at both stations. This leads to a serious overestimation of the albedo which in turn produces the error in the net shortwave radiation.

## 3.4 Energy Balance

The variation of the incoming shortwave radiation with height was not taken into account because it depends for the most part on the model's forecast of cloud heights. The impact of changes in cloudiness are dramatically reduced over surfaces with high albedos because of multiple reflections between the cloud base and the surface (Schneider and Dickinson, 1976). Fig.7 shows the downwelling shortwave radiation at Thule ($11\,m.$) located on the coast in Greenland and South Pole station ($2835\,m.$) in Antarctica. The annual cycle of the downwelling shortwave radiation is generally well simulated, both climate models do however exhibit a tendency to underestimate the peak intensity of summer insolation.

The downwelling longwave radiation derived from the MIT climate model output is in-

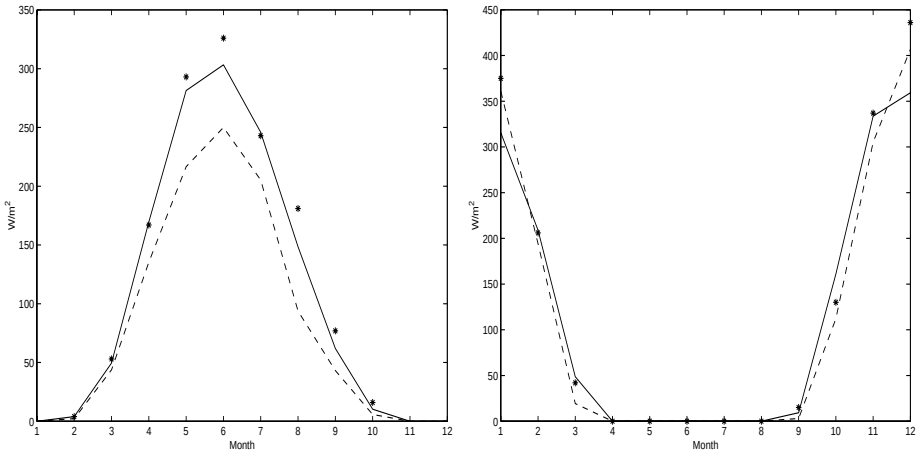


Figure 7: Seasonal variation of the downwelling shortwave radiation at the Thule ($76°31'N; 68°50'W; 11\ m$,Greenland) and South Pole ($1850\,m.$, Antarctica) stations. Full line: MIT model, Dashed line: ECHAM model, $*$: observations. Source for the observed is Gilgen and Ohmura (1999).

terpolated linearly between the model levels to the altitude of the grid points on the ice sheet, the values predicted by the ECHAM model are left unaltered. Neither climate model appears to have any systematic biases in estimating this component of the radiation balance (not shown).

Because the upwelling longwave radiation flux depends only on the surface snow or ice temperature (blackbody emission, the emissivity of snow and ice is very close to one in the infrared part of the spectrum), which is in turn determined by the net surface energy budget, the upwelling longwave radiative flux provides a very good indicator of the overall quality of that budget. The comparison (Fig. 8) between observations and model estimates at ETH Camp ($1155\,m.$) for Greenland and South Pole ($2835\,m.$) for Antarctica shows that the agreement is generally good, although the model's tendency to underestimate the peak insolation can lead to surface snow temperatures which are too cold and an underestimation of the upwelling longwave flux (this occurs for example at the Carrefour site, not shown). In the summer in the ablation zone this flux is constrained by the surface ice temperature which remains near the melting point. The agreement between the model predictions and the station data at lower elevations in Greenland is therefore also very good.

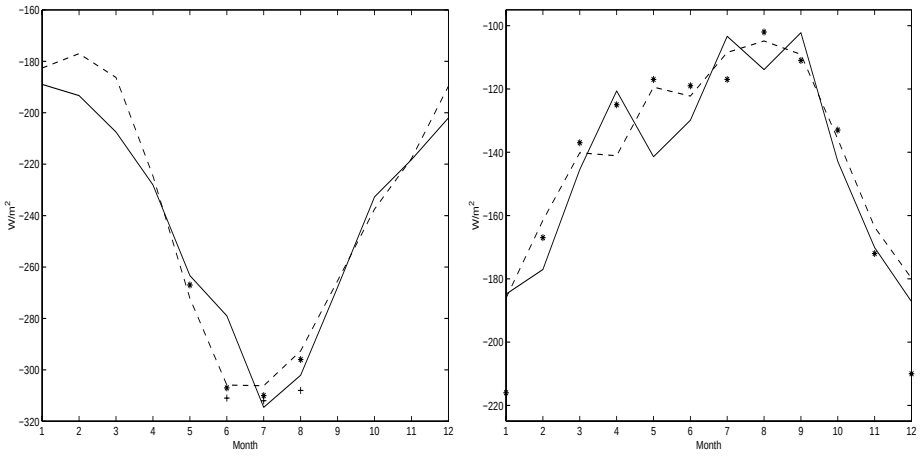


Figure 8: Seasonal variation of the upwelling longwave radiation at ETH Camp ($69°34'N; 49°17'W; 1155\ m$, Greenland) and South Pole station ($1850\,m.$, Antarctica). Full line: MIT model, Dashed line: ECHAM model, $*$: observations. Source for the observed is Gilgen and Ohmura (1999).

There exist few reliable measurements of the turbulent latent and sensible heat fluxes to compare the model's output with, most published estimates are themselves derived from bulk formulae and therefore depend on the details of those parameterizations. The model's relative humidity was chosen to give a good aggreement with the measurements taken at ETH Camp.

# 4 Performance of the Combined Climate and Snow Melt Models

The six possible combinations of climate and melt models are tested by comparing the predicted ablation to measurements taken at stakes drilled into glaciers on the ice sheet. These surface measurements do not account for the refreezing of meltwater within the snow cover or the glacier, it is therefore more appropriate to compare them to the melting predicted by the snowpack model than to the runoff value. The two climate / snowpack models are furthermore tested by comparing the predicted extent of the wet snow zone to satellite measurements.

## 4.1 Ablation at Individual Stations

An example of the seasonal evolution of the different elements composing the local mass balance of the snow cover at Qamanârssûp Sermia produced with the MIT model input and the snowpack model is shown in Fig.9. The random variability added to the temperature distribution leads to concurrent rain- and snowfall in the spring and fall. The slight shift towards the fall of the seasonal distribution of runoff when compared to observations is due to the underestimation of the downwelling shortwave radiation by the model in June. The excess runoff in July is most likely linked to a slight overestimation of the air temperature, and thus underestimation of the albedo, during that month. The seasonal variation in the amount of meltwater which refreezes reflects the energy which is spent in the spring to bring the snowpack to the melting point and the drop in temperatures in the fall which is sufficient to refreeze part of the meltwater present within the snow. Once ice is exposed at the surface during the summer, the potential for refreezing is eliminated and the meltwater becomes runoff. The observed ablation at Qamanârssûp Sermia is 3.50 $m$, the MIT / snowpack model combination predicts 3.21 $m$. The average summer temperature at that station is $5.4°C$, which leads the linear model to predict 3.56 $m$ of ablation. There are four months with temperatures above the melting point, for a total of 527 positive degree-days. Only 19 PDD's are necessary to melt the winter's snowfall, the remainder is used to melt ice for a total runoff of 4 $m$.

The runoff predicted by the six model combinations is compared, in Table 3, to observations at the few stations which provide that information. The MIT model combined with the snowpack or the PDD model provides the best estimates of ablation in the Southern two-thirds of the ice sheet (first four stations on the list). The underestimation of runoff at ETH Camp is linked to the downwelling shortwave radiation being slightly too small, the excess runoff at Nordbogletscher is due to the model's mid-summer air temperatures being slightly too warm. The largest discrepancies between these two model combinations occurs at Camp 4 and the absence of ablation measurements at that station does not allow any inferences from this difference. One can however expect the models to diverge for average summer temperatures higher than those experienced at these four stations: While the runoff

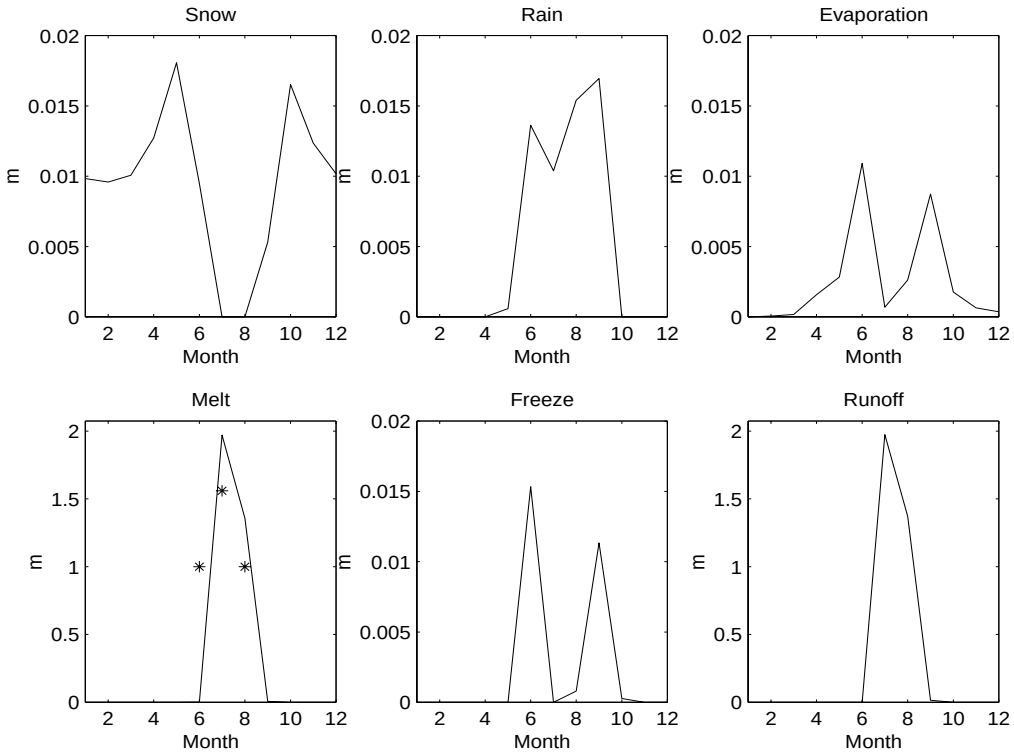


Figure 9: Snowfall, rainfall, melting, freezing, runoff and evaporation at Qamanârssûp Sermia ($64°28'N; 49°50'W; 790\ m$, Greenland), in $m$ predicted by the MIT / snowpack model combination. The $*$ are observations, Braithwaite & Olesen, 1989.

predicted by the PDD model grows linearly as summer temperatures increase, the amount of meltwater generated by the snowpack model is a function of the surface energy balance. The latter has a much weaker dependence on the air temperature once the winter's snow is melted and ice is exposed at the surface.

The equilibrium line – the elevation at which annual accumulation and ablation are balanced – is placed at approximately the correct elevation by the MIT-PDD/snowpack model combinations, near ETH Camp and Camp 4 EGIG in Greenland and off the coast in Antarctica. Regional variations in climate such as those distinguishing Nordbogletscher and Qamanârssûp Sermia, which are responsible for the difference in ablation between those two stations are not captured by the coarse resolution of the MIT climate model.

Although refreezing is a small quantity in the example shown in Fig.9 for Qamanârssûp Sermia, it plays an important role near the equilibrium line of the Greenland ice sheet,

| | MIT | | | ECHAM 4 | | | Observations |
|---|---|---|---|---|---|---|---|
| Station | Snowpack | PDD | Linear | Snowpack | PDD | Linear | |
| ETH Camp | 24 | 54 | 101 | 14 | 131 | 165 | 40[†] |
| Camp 4 EGIG | 23 | 102 | 148 | 16 | 142 | 229 | |
| Nordbogletscher | 363 | 369 | 361 | 0 | 0 | 73 | 250[‡] |
| Qamanârssûp | 321 | 400 | 356 | 36 | 90 | 210 | 350[‡] |
| Kronprins Christian L. | 0 | 0 | 99 | 0 | 53 | 132 | Jul 8-27 1993:80[§] |
| Storstrømmen | 5 | 7 | 157 | 159 | 367 | 372 | $\sim 200$[¶] |

Table 3: Comparison between the ablation predicted by the six model combinations and observations at ETH station ($69°34'N; 49°17'W; 1155\ m$), Camp 4 EGIG ($69°40'N; 49°37'W; 1004\ m$), Nordbogletscher ($61°28'N; 45°20'W; 880\ m$), Qamanârssûp Sermia ($64°28'N; 49°50'W; 790\ m$), Kronprins Christian Land ($79°54'N; 24°04'W; 380\ m$), Storstrømmen ($77°10'N; 20°20'W; 230\ m$); all on the Greenland ice sheet. Source for the observed: [†]: Ohmura et al. (1992). [‡]: Braithwaite and Olesen (1990). [§]: Konzelmann and Braithwaite (1995). [¶]: Bøggild et al. (1994). Units are $cm$.

for example at Camp 4 EGIG or ETH Camp, or in Antarctica. Refreezing would also be responsible for delaying the effect of the warming of air temperatures on runoff: As the melt zone expands, the firn thickness which has to be brought to the melting point before any runoff can occur increases. The bulk of the extra energy would thus go at first into forming superimposed ice layers within the firn before any runoff could begin to take place. This effect is particularly noticeable during the model spinup (which begins with a prescribed density profile which increases linearly from 320 $kg\,m^{-3}$ at the surface to 600 $kg\,m^{-3}$ at 15 $m$ depth): the amount of refreezing taking place at Qamanârssûp Sermia drops from about $30\,cm$ to it's equilibrium value of 3 $cm$ over the 150 years of the spinup.

The MIT / linear model combination's estimates of ablation are only adequate where the average summer temperature is predicted very accurately, namely at Qamanârssûp Sermia. An error of $2°C$ on the climate model's part leads to a difference of $1m$ in the predicted ablation. This is an accuracy which regional climate predictions have yet to attain.

The ECHAM model was shown in the previous section to underestimate the surface air

temperature at Nordbogletscher and Qamanârssûp Sermia, this in turn leads the melt models to underestimate the ablation. The warmer summer temperatures of the ECHAM model in the Northern half of the ice sheet induce melting and runoff at Kronprins Christian Land and Storstrømmen, which the MIT model fails to capture. While the MIT / snowpack and ECHAM / snowpack models give similar results at ETH Camp, the slightly warmer summer temperatures of the ECHAM model lead to large differences in the ablation predicted by the PDD and Linear models, which both overestimate the ablation. This discrepancy highlights the danger of relying on a single model input, temperature, to calculate runoff.

## 4.2 Extent of the Wet Snow Zone

The ability of the combined climate / snowpack models to reproduce the current climate was tested by comparing the predicted extent of the "wet snow" zone to the same quantity derived from passive satellite microwave remote sensing measurements over Greenland and Antarctica (Abdalati and Steffen, 1997; Zwally and Fiegles, 1994). The satellite measurements do not give any quantitative information about the amount of liquid water present in the firn, but simply indicate whether the snow is wet or dry depending on its surface reflectivity. The shading in Fig.10 indicates the percentage of days during each of the three summer months when the pixel was wet. This information can be reproduced by the snowpack model because it disaggregates the monthly mean climatic input into time series of temperature and precipitation. The model's grid point is considered wet if rainfall or melting has occurred during the preceeding time period and liquid water is present at the surface. It is not possible to reproduce this information with the linear model which calculates only ablation.

The results obtained with the snowpack model and the MIT climate are shown as the top panels of Fig.10, the ECHAM model results form the bottom panels, the three columns represent respectively June, July and August. Fig.10 is directly comparable to Fig. 4 of Abdalati and Steffen (1997). While the ECHAM model produces intense melting mostly along the western and northern coast of Greenland throughout the summer, the extent of the wet snow zone predicted by the MIT model is concentrated in the southern half of

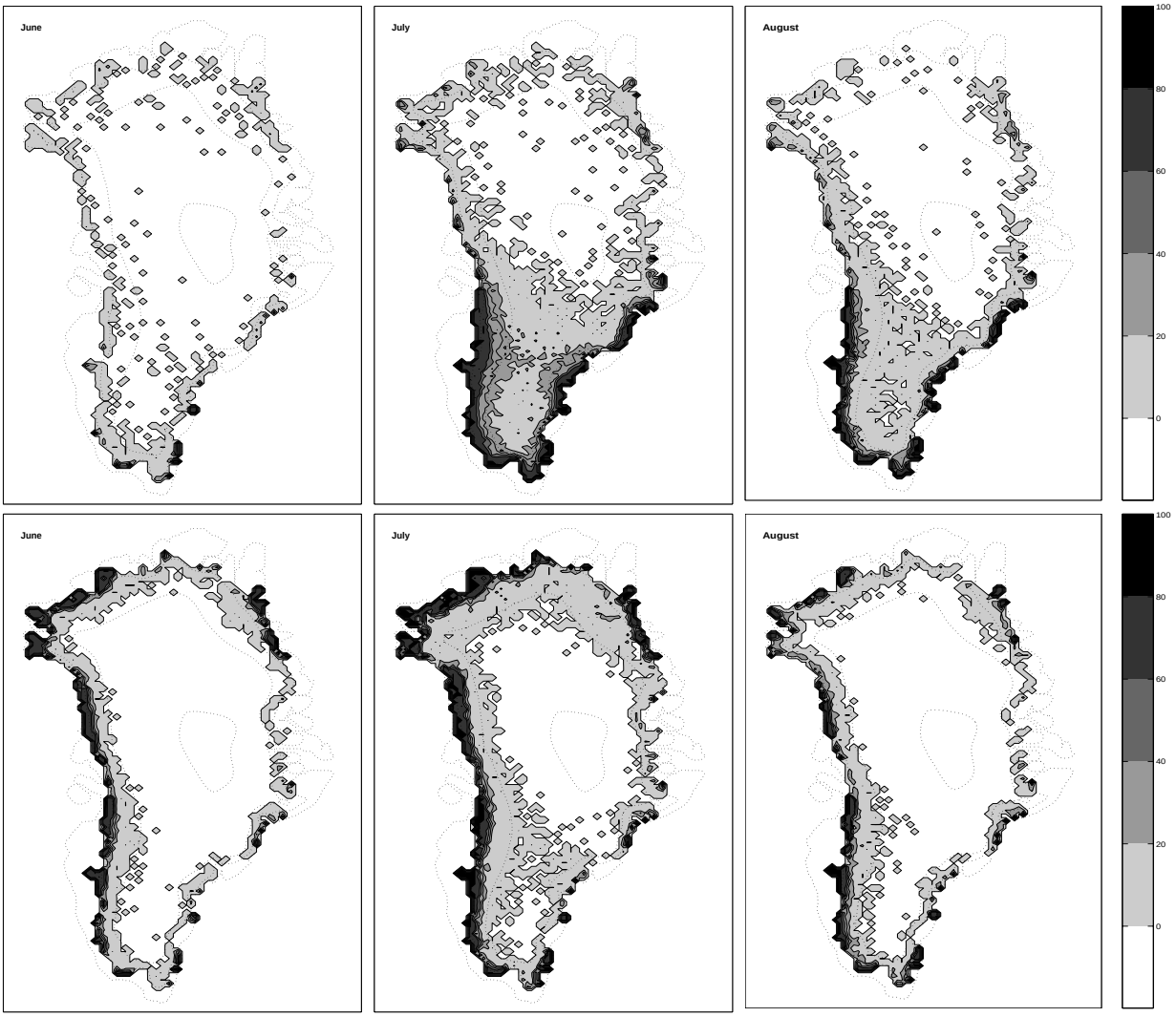


Figure 10: Model derived extent of the melt zone during the three summer months on a 20 $km$ grid. Top: MIT / snowpack model, Bottom: ECHAM4/snowpack model. Left: June, Middle: July, Right: August. Note that the land covered areas are shown in white. Dotted lines are 1000 $m$. topographic height contours.

the ice sheet and extends further inland. Except for June when the extent of melting is underestimated, both the areal extent and intensity (in terms of % of days which experience melting) of the melting predicted by the MIT / snowpack model match observations fairly closely. This indicates that the total ablation predicted by this model for the entire ice sheet can be viewed as a conservative estimate of the total runoff originating from the Greenland ice sheet. The ECHAM model reproduces the observed melting along the northern coast which is not captured by the MIT model but fails to reproduce the areal extent of the wet snow zone in the southern half of the ice sheet where most of the melting occurs. This in turn leads this model combination to underestimate the total runoff when compared to observations.

The extent of the wet snow zone for Antarctica predicted by both climate / snowpack models is shown in Fig.11, it can be compared to the observations by Zwally & Fiegles for the 1982/83 and 1983/84 summers, their Fig. 4. Since 1982/83 saw unusually high surface melting, and 1983/84 below average surface melting, the model predictions will be compared to the average of those two years. The Antarctic Peninsula usually experiences 50–60 days of melting, the MIT model sees only 40–50% of the summer or a total of 35-45 days with surface melt, the ECHAM model only 20–40% or 18–35 days during the summer. The rest of the coast (the ice shelves which are floating ice masses are excluded from the model predictions) experiences on average less than 20 days of melting which compares favorably with the 20–40% (18-36 days) predicted by the MIT model. The ECHAM model fails to give any surface melting anywhere but on the Peninsula and in the South-Western quadrant. The areal extent of the melt zone predicted by the MIT model is therefore closer to observations than that predicted by the ECHAM model. Note that virtually all of this rain and meltwater refreezes in situ and neither model combination predicts any runoff originating from the Antarctic ice sheet.

The degree-day model produces a wet snow zone generally slightly smaller than that of the snowpack model, but which generally shares the same features.

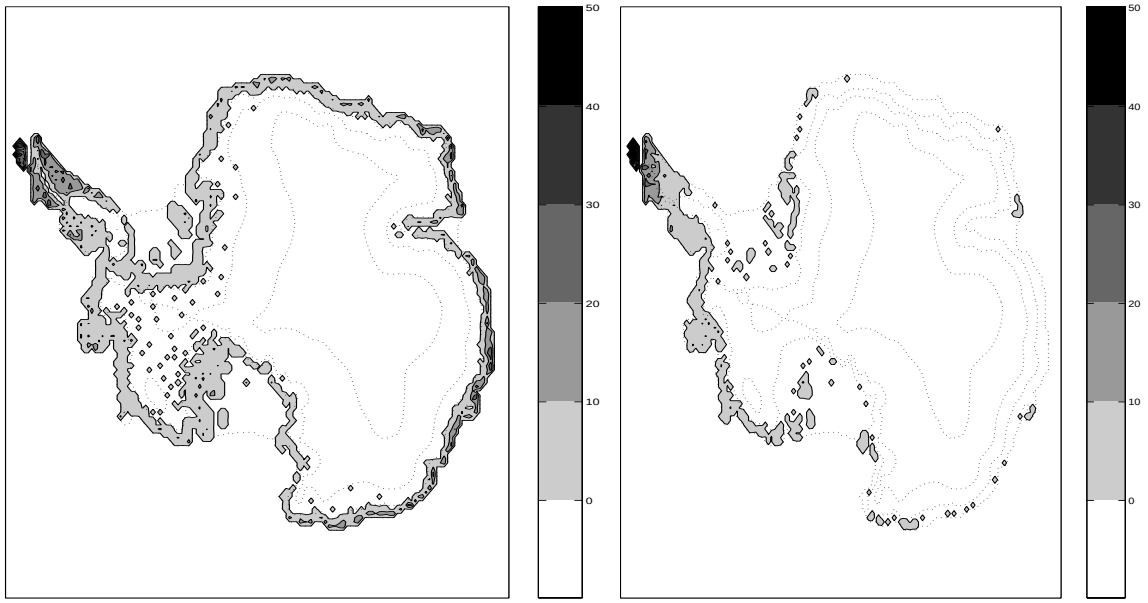


Figure 11: Model derived extent of the melt zone during the three summer months (December, January, February). Left: MIT / snowpack model, Right: ECHAM / snowpack model. Dotted lines are the $1000\,m.$ topographic height contours. The shading represents the % of days which experienced melting during the summer.

# 5 Ablation on the Greenland and Antarctic Ice Sheet

The maps in Fig.12 show the runoff from the Greenland ice sheet as calculated on a $20\,km$ grid with the three models described in section 2, the figures in the left-hand column used the MIT climate model input while the right-hand column used the ECHAM data as model input. Table 4 summarizes the maps by comparing the total runoff originating from the Greenland ice sheet to Reeh's (Houghton et al., 1996) estimate derived from observations. Note that the measurements of runoff are highly uncertain: Paterson (1994) suggested adding error bars of $\pm 100 \cdot 10^{12}\,kg\,a^{-1}$ onto these numbers.

Of the three versions which use the MIT climate model, the linear model produces the largest source area of runoff, followed by the snowpack and the PDD versions. The PDD model compensates by predicting more intense melting and runoff than the snowpack model at certain locations: Maximum runoff values are $\sim 7\,m$ near the southeastern coast of the island instead of $5.5\,m.$ and slightly more than $5\,m$ on the western side instead of the $3-4\,m.$

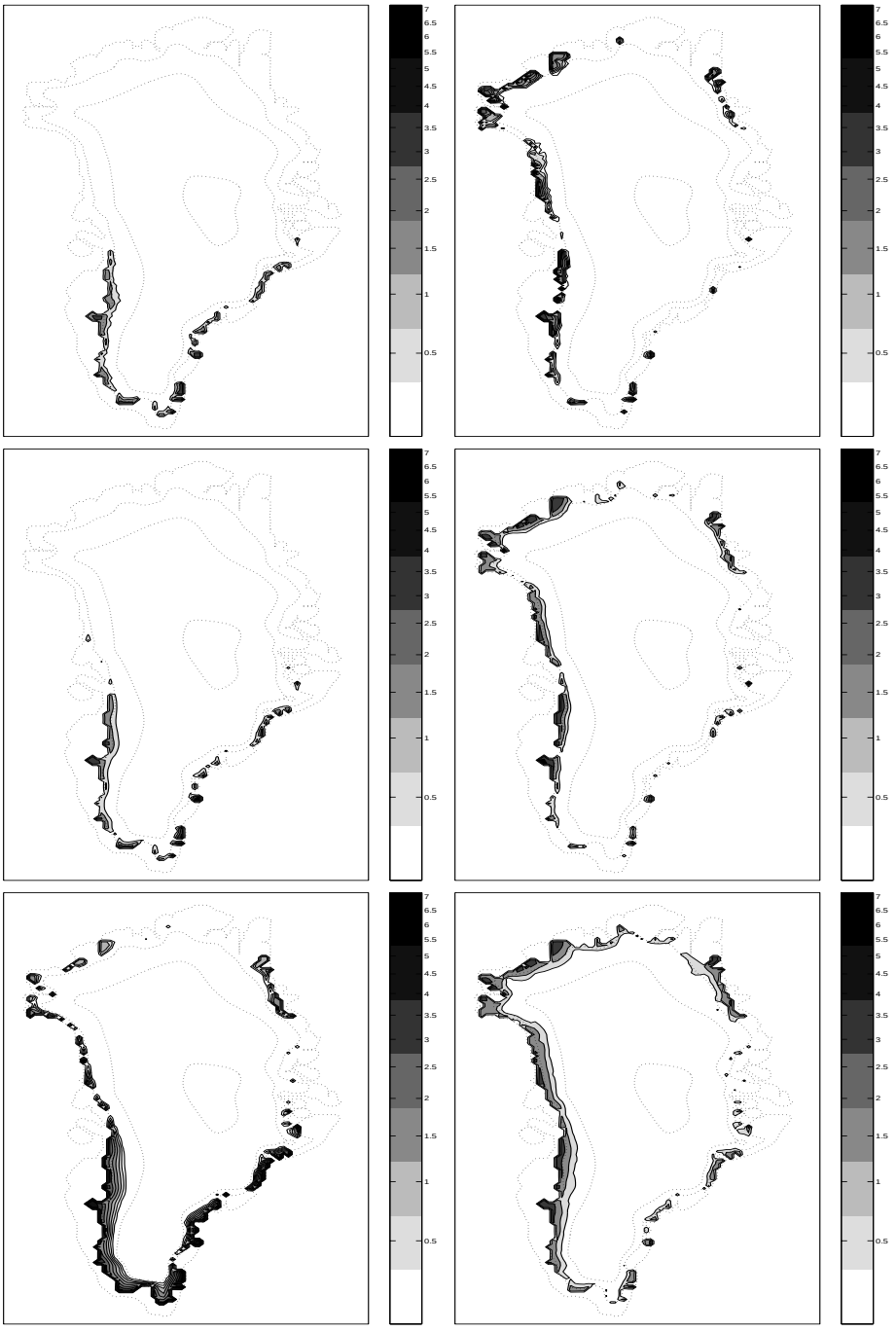


Figure 12: Runoff in $m\,year^{-1}$. Left column: MIT climate model, Right column: ECHAM model. Top row: Snowpack model, Middle row: Positive Degree-Day model, Bottom row: Linear model. Dotted lines are the $1000\,m.$ topographic height contours.

| | MIT | | | ECHAM 4 | | | Observations |
|---|---|---|---|---|---|---|---|
| | Snowpack | PDD | Linear | Snowpack | PDD | Linear | |
| Greenland - 40 $km$ | 203 | 235 | 364 | 93 | 396 | 668 | 237 |
| Greenland 20 $km$ | 162 | 172 | 299 | 122 | 353 | 568 | |
| Antarctica - 40 $km$ | 0 | 63 | 620 | 0 | 18 | 122 | 53 |

Table 4: Runoff from the Greenland and Antarctica ice sheets calculated with the Snowpack, Positive Degree-Day (PDD) and Linear methods. Source for the observations are Houghton et al. (1996). Units are $10^{12}\, kg\, year^{-1}$

predicted by the snowpack model. The maximum values predicted by the linear model are in agreement with those of the snowpack model.

The aggregate estimates are shown to depend strongly upon the model resolution, with runoff decreasing by $\sim 20\%$ as the grid size is halved. Figure 13 shows the difference in the extent of the source area of runoff when the resolution is doubled. This effect has been noted by Glover (1999) who attributed it to the strongly sloping margins of the Greenland coastline. According to that study, increasing the resolution beyond a $0.5° \times 0.5°$ grid ($\sim 20 \times 50\, km$ at $70°N$) no longer changes the estimations of runoff, the results obtained with the finer grid can therefore be trusted as being independent of the model resolution.

The aggregate estimates produced with the snowpack and the PDD model combinations are within 10 – 15 % of each other and 25 – 30 % lower than the observed value, the linear model predicts ∼70 – 80 % more runoff than the snowpack model and 30% more than observed. Because one method relies on the surface energy balance to determine the amount of melting while the other two rely only on air temperature, the reasonable agreement between these methods is reassuring as to the internal consistency of the input climate data and as to the reliability of the predictions. Note that because the MIT / snowpack model underestimates the extent of the wet snow zone along the northern coast, the $162 \cdot 10^{12}\, kg\, a^{-1}$ most likely underestimates the total runoff.

The three model versions which used the ECHAM model data as input give substantially different results. There is a significant area of the ice sheet which experiences average summer

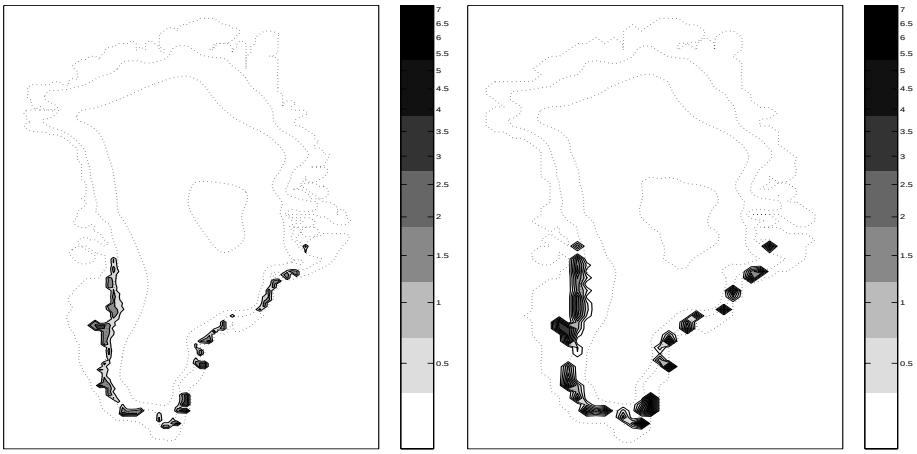


Figure 13: Runoff in $m\,year^{-1}$ predicted by the MIT / snowpack model combination. Left panel: MIT 20 $km$ resolution, Right panel: MIT 40 $km$ resolution. Dotted lines are the 1000 $m$. topographic height contours.

temperatures in the -2 – 0°$C$ range, thereby explaining the difference between the PDD model which ablates only for air temperatures above the melting point and refreezes the initial portion of meltwater and the linear model which predicts runoff starting at air temperatures of $-2°C$. Both temperature based methods predict significantly more ablation than the model based on the energy budget which has the ability to refreeze a significant portion of the meltwater which is formed, $\sim 40\%$ or $49 \cdot 10^{12}\,kg/a$, in particular in the Northern half of the ice sheet. This leads to a relatively low estimate for the total runoff of $122 \cdot 10^{12}\,kg/a$. In comparison, the MIT / snowpack model combination refreezes only $\sim 20\%$ or $35 \cdot 10^{12}\,kg/a$ of the meltwater which is generated.

The snowpack model refreezes in-situ all the melt- or rainwater which accumulates at the surface of the Antarctic ice sheet. This is in large part due to the strongly negative energy budget during the winter months which is responsible for the low temperatures of the snow and firn. A significant amount of energy can therefore be added to the firn as latent heat released by the freezing process before any runoff can take place. The degree-day model accounts to some degree for refreezing and predicts only a minimal amount of runoff. The linear model however generates runoff as soon as the average summer temperature reaches $-2°C$ which includes a large portion of the Antarctic Peninsula and areas along the coast

in the $45 - 135° E$ quadrant. Although not entirely impossible and not inconsistent with the melt extent presented by Zwally and Fiegles (1994) , the predicted runoff of $620 \cdot 10^{12}$ (MIT) and $122 \cdot 10^{12} kg\, a^{-1}$ (ECHAM) is much larger than the estimates derived from measurements which are thought to be close to $50 \cdot 10^{12}\, kg\, a^{-1}$ (Houghton et al., 1996). Because melting is currently limited to coastal areas, it is possible that a higher resolution than the $40\, km$ grid which was used could change the estimate of runoff.

# 6 Discussion

Although simpler than a sophisticated three-dimensional GCM, the MIT model's climate input coupled to the snowpack model does a respectable job at capturing the known features of the melting and ablation which occur on the Greenland and Antarctic ice sheets. More measurements of the radiative fluxes, temperature and ablation would however be necessary to affirm this with certainty. The estimate of $162 \cdot 10^{12}\, kg\, a^{-1}$ of runoff produced with the MIT / snowpack model combination for Greenland does underestimate the actual ablation because of the absence of runoff along the Northern coast of the ice sheet. A significant portion of the meltwater refreezes within the snow cover to form superimposed ice layers in both the MIT / snowpack and ECHAM / snowpack model combinations, yet the fraction of meltwater which ends up as runoff is significantly different in both cases. This highlights the advantage of an explicit calculation of the liquid water content of the snow cover and of changes of phase of water over a parameterization. The degree-day model in the formulation used for this study provides an adequate first approach to modeling the mass balance of the ice sheets. One must however be excessively careful in using temperature based parameterizations such as the degree-day or linear models in regions other than those for which they were calibrated and for climatic forcings different from the current state. This will become clear in climate change simulations (Bugnion, 1999). The linear model furthermore fails to recognize the non-linear dependence of melting and runoff on the surface albedo, and the role of refreezing.

The summer temperature pattern predicted by the ECHAM model for the Greenland ice sheet is not sufficiently accurate to give reasonable estimates of runoff. The failure of the ECHAM model to improve the estimates provided by the MIT model is particularly

disappointing in view of the extremely high resolution of the simulation which served as input, a resolution which could not be sustained in a transient climate change integration. This does however confirm that regional predictions from GCMs cannot yet be fully trusted. The high resolution of the ECHAM model does however allow it to improve the accuracy of the pattern and amount of snow accumulation on both ice sheets, the excessive accumulation over Antarctica being the major shortcoming of the MIT model. Since that climate model is likely to continue overestimating precipitation in integrations carried out over the $21^{st}$ century, this is a problem which could be particularly detrimental to the reliability of estimates of future changes in the mass balance of that ice sheet and their effect on the level of the oceans.

These calculations were designed to gain confidence in the ability of the coupled climate / snowpack model to capture the current state of the mass balance of the ice sheets before proceeding with the calculation of the changes which can be expected to occur in the coming century and their effect on the sea-level. The simple MIT climate model coupled to a sophisticated snowcover model seems to give an accurate prediction of the melting and runoff on the Greenland ice sheet, probably the variable which is the most difficult to estimate. A subsequent paper Bugnion (1999) looks into changes in mass balance of Greenland and Antarctica over the coming century for a range of climate change scenarios sufficiently broad to capture the major uncertainties in the rate of emissions of greenhouse gases and in key parameters in the climate model. This allows to calculate a set of projections of the changes in sea-level which follow from these modifications in the mass balance.

## Acknowledgements

I am grateful to the ETH Zürich (Prof. A. Ohmura, Dr. H. Gilgen, Dr. M. Wild, ) for providing the ECHAM 4 and GEBA sdata. Insightful coments on earlier drafts were provided by G. Roe, P. Stone and M. Wild. This research was supported by the Alliance for Global Sustainability, the M.I.T. Joint Program on the the Science and Policy of Global Change and NASA Grant NAG 5-7204 as part of the NASA GISS Interdisciplinary EOS Investigation.

# References


Abdalati, W. and K. Steffen. 1997. Snowmelt on the Greenland ice sheet as derived from passive microwave satellite data. *J. Climate*, **10**(2), 165 175.

Anderson, E. 1976. A point energy and mass balance model of the snow cover. Technical Report NWS 19, NOAA, Office of Hydrology, National Weather Service, Silver Spring, Md.

Bader, H.-P. and P. Weilenmann. 1992. Modeling temperature distribution, energy and mass flow in a (phase-changing) snowpack. I. Model and case studies. *Cold Regions Science and Technology*, **20**, 157 181.

Bøggild, C., N.Reeh, and H. Oerter. 1994. Modelling ablaiton and mass-balance sensitivity to climate change of Storstrømmen, Northeast Greenland. *Global and Planetary Change*, **9**, 79 90.

Braithwaite, R. and O. B. Olesen. 1989. Calculation of glacier ablation from air temperature, West Greenland. In Oerlemans, J., *ed.*, *Glacier Fluctutations and Climatic Change*, 219 233. Kluwer Academic, Dordrecht.

Braithwaite, R. and O. Olesen. 1990. A simple energy-balance model to calculate ice ablation at the margin of the Greenland ice sheet. *J. Glaciol.*, **36**(123), 222 228.

Braithwaite, R. J. 1995. Positive degree-day factors for ablation on the Greenland ice sheet studied by energy-balance modelling. *J. Glaciol.*, **41**(137), 153 159.

Brun, E., E. Martin, V. Simon, C. Gendre, and C. Coleou. 1989. An energy and mass model of snow cover suitable for operational avalanche forecasting. *J. Glaciol.*, **35**(121), 333 342.

Bugnion, V. 1999. Changes in mass balance of the Greenland and Antarctic ice sheets over the $21^{st}$ century. *Submitted to J. Geophys. Res.*

Colbeck, S. C. 1972. A theory of water percolation in snow. *J. Glaciol.*, **11**(63), 369 384.

Genthon, C. 1994. Antarctic climate modeling with general circulation models of the atmosphere. *J. Geophys. Res.*, **99**(D6), 12953 12961.

Gilgen, H. and A. Ohmura. 1999. The global energy balance archive (GEBA). *Bulletin of the American Meteorological Society*, **80**(5), 831 850.

Glover, R. 1999. Influence of spatial resolution and treatment of orography on GCM estimates of the surface mass balance of the Greenland ice sheet. *J. Climate*, **12**(2), 551 563.

Greuell, W. 1992. Numerical Modelling of the Energy Balance and the Englacial Temperature at the ETH Camp, West Greenland. Technical Report 51, Zürcher Geographische Schriften, ETH Zürich.

Hansen, J. et al. 1983. Efficient three dimensional global models for climate studies. *Monthly Weather Review*, 609 662.

Houghton, J., L. Filho, B. Callander, N. Harris, A. Kattenberg, and K. maskell, *eds.* 1996. *Climate Change 1995: The Science of Climate Change*. Cambridge University Press.

Huybrechts, P., A. Letréguilly, and N. Reeh. 1989. The Greenland ice sheet and greenhouse warming. *Palaeogeography, Palaeoclimatology, Palaeoecology*, **89**, 399 412.

Kang, E. 1994. Energy-Water-Mass Balance and Hydrological Discharge. Technical Report 57, Zürcher Geogrphische Schriften, ETH Zürich.

Knap, W. and J. Oerlemans. 1996. The surface albedo of the Greenland ice sheet: satellite derived and in situ measurements in the Söndre Strömfjord area during the 1991 melt season. *J. Glaciol.*, **42**, 364 374.

Konzelmann, T. and R. Braithwaite. 1995. Variations of ablation, albedo and energy balance at the margin of the Greenland ice sheet, Kronprins Christain Land, eastern north Greenland. *J. Glaciol.*, **41**(137), 174 181.

Loth, B. and H.-F. Graf. 1993. Snow cover model for global climate simulations. *J. Geophys. Res.*, **98**(D6), 10451 10464.

Male, D. H., 1980. *Dynamics of Snow and Ice Masses*, chapter The Seasonal Snowcover, 305 395. Academic Press.

Morland, L., R. Kelly, and E. Morris. 1990. A mixture theory for a phase-changing snowpack. *Cold Regions Science and Technology*, **17**, 271 285.

Morris, E., H.-P. Bader, and P. Weilenmann. 1997. Modelling temperature variations in polar snow using DAISY. *J. Glaciol.*, **43**(143), 180 191.

Ohmura, A. et al. 1992. ETH Greenland Expedition. Progress Report No. 2: April 1991 to October 1992. Technical report, Department of Geography, ETH Zürich.

Ohmura, A. 1987. New temperature distribution maps for Greenland. *Z. Gletscherkd. Glazialgeol.*, **23**(1), 1 45.

Paterson, W. *The Physics of Glaciers*. Pergamon, $3^{rd}$ edition.

Roeckner, E., L. Bengtsson, J. Feichter, J. Lelieveld, and H. Rodhe. 1999. Transient climate change simulations with a coupled atmosphere-ocean GCM including the tropospheric sulfur cycle. *J. Climate*.

Schneider, S. H. and R. E. Dickinson. 1976. Parameterization of fractional cloud amounts in climate models: The importance of multiple reflections. *J. Appl. Meteor*, **15**, 1050 1056.

Schwerdtfeger, W., 1970. *World Survey of Climatology*, chapter 4. Elsevier, The Climate of the Antarctic.

Sokolov, A. and P. Stone. 1995. Description and validation of the MIT version of the GISS 2D model. Technical Report 11, Joint Program on the Science and Policy of Global Change, MIT.

Sokolov, A. P. and P. H. Stone. 1998. A flexible climate model for use in integrated assessments. *Clim. Dyn.*, **14**(4), 291 303.

Vaughan, D., J. Bamber, and M. Giovinetto. 1999. Reassessment of net surface mass balance in Antarctica. *J. Climate*, **12**(4), 933 946.

Wild, M. and A. Ohmura. 1999. Effects of polar ice sheets on sea-level in high resolution greenhouse scenarios. *Submitted to Geophys. Res. Lett.*

Zwally, H. and S. Fiegles. 1994. Extent and duration of Antarctica surface melting. *J. Glaciol.*, **40**(136).